LONDON, METEOROLOGICAL OFFICE.

Met.O.15 Internal Report No.47.

Analysis of the liquid water content distribution in cumuliform cloud for helicopter icing studies. By BROWN,R. and McADAM,M.

London,Met.Off.,Met.O.15 Intern.Rep.No.47, 1982,32cm.Pp.14,15 pls.5 Refs.

An unofficial document - not to be quoted in print.

METEOROLOGICAL OFFICE
London Road, Bracknell, Berks.

MET.O.15 INTERNAL REPORT

No 47

Analysis of the liquid water content distribution in cumuliform cloud for helicopter icing studies

by

R Brown and M McAdam

Cloud Physics Branch (Met.O.15)

December 1982

LF

1. Introduction

The contribution of the Cloud Physics Branch (Met O 15) to the Helicopter Icing Studies involves specifying the distribution of liquid water content in various cloud types, as a function of height above cloud base and/or temperature. Measurements made from the C-130 of the Meteorological Research Flight form the basis of this work. The first phase concentrated on non-precipitating, non-glaciated layer cloud and has been completed apart from the production of a final report. Some of these clouds had base temperatures above $0^{\circ}C$. By using the adiabatic concept measurements made at temperatures above $0^{\circ}C$ can be related to supercooled cloud, since it can be argued that the cloud dynamics determines the departure from adiabatic liquid water contents, not the temperature. This assumption will be invalidated by significant glaciation so that the results will only be applicable to Sc/St.

The second phase has involved undertaking a similar study for cumuliform cloud. A significant quantity of data in Cu has been gathered for other projects and it was decided to analyse a sample of this before undertaking further specific flights for icing studies. Besides the intrinsic value of this data it was felt that the analysis would inform the development of flight plans for further icing studies. Data from three days has been analysed in terms of the adiabatic concept. The observations encompass a wide variety of conditions including precipitation and glaciation. The results of the analysis are described in this report together with a description of the difficulties encountered.

The information on the distribution of liquid water content is used by the Special Investigations Branch (Met O 9), in conjunction with synoptic data on the distribution of cloud, to quantify the probability of encountering specified values of supercooled liquid water content. In order to complete a preliminary analysis on a reasonable time scale Met O 9 have used measurements made in the USSR and summarised in Khrgian (1963). He has classified liquid water contents by temperature only, ignoring variations with height above cloud base. Such an approach takes account of the affects of glaciation but may produce unrealistic values near cloud base. Met O 9 have allowed for this by imposing a zero probability for superadiabatic liquid water content. Khrgian has summarised a large body of data but its quality is unknown. Met O 15 have obtained less data but it is likely to be of a higher quality. Therefore it was decided to treat the Russian data as a hypothesis to be examined by our results. A program has been written to classify the liquid water contents by temperature alone and the results from this are also described.

2. Instrumentation

Liquid water contents were measured with a Johnson-Williams liquid water content meter (J-W). The Meteorological Office J-W system performed well during trials in the icing tunnel operated by the Low Temperature Laboratory of the National Research Council of Canada as described by Strapp and Schemenauer (1982). Unfortunately they do not indicate the origin of the instruments tested. However our records show that both our J-W's agreed with the tunnel liquid water contents to within five per cent. Personne et al (1982) have compared the power spectrum of the J-W signal with that from a Ruskin Probe. They found that the J-W has a cutoff frequency (Fc) close to 0.4 Hz (response time $t = (2\pi f_c)^{-1} \simeq 0{\cdot}4\,s$) above which the signal is attenuated by 20 dB per decade. The basic analysis has been performed using 1 s mean J-W liquid water contents representing a spatial average over 100 m.

Cloud droplet spectra were measured using an Axially Scattering Spectrometer Probe (ASSP-100). In addition particles in the diameter range 25 to 6400 μm were sized using 2-D OAP Cloud and Precipitation Probes. The image produced by these can be identified as a water drop or ice crystal provided the diameter exceeds about 200 μm.

3. KONTUR Flight H463 23 September 1982

3.1 Meteorological Situation and Flight Plan

On this day a ridge moved eastwards over the North Sea ahead of a front approaching the British Isles from the West. Early in the day a trough was apparent over the Eastern North Sea. The observational area (around 55°N, 6°E) contained many small Cu with an occasional large Cu or Cb.

The KONTUR flight plan consisted of a series of L's, 78 x 100 nm flown at different heights together with three profiles. The profiles were normally performed at the extremities of the L with an additional profile roughly halfway along the diagonal joining the extremities.

3.2 Specification of Cloud Base Height

Whilst the long horizontal legs of the KONTUR flight plan are useful in providing enough liquid water content values for statistical analysis, they do not provide sufficient information on cloud base height, since only three profiles are included. During a profile descent the aircraft scientist estimated when the aircraft was at cloud base and noted the height from a pressure altimeter. The reported cloud base heights are required by the analysis program to calculate the adiabatic liquid water content. The analysis program

calculates heights using the pressure recorded from a different altimeter to that read by the aircraft scientist. Since the two altimeters are not necessarily set to the same surface pressure a correction is applied to the reported cloud base heights. On this day 40 m was added to the profile 1 and 2 base heights and 17 m to profile 3 giving base heights of 590, 500 and 690 m respectively.

A constant cloud base height has been specified for each leg. The analysis program calculates the height for each data point from the recorded pressure assuming a constant surface pressure, surface temperature and lapse rate. Errors caused by variations in the latter two parameters are negligible. However the surface pressure increased by 4 mb along one leg of the L and decreased by 1 mb along the other leg. No correction has been applied for this since the maximum error of 40 m lies within the anticipated error in cloud base height.

In order to extend the sparse information on cloud base, a program has been written to estimate the cloud base height and temperature from the peak liquid water content observed during a specified period. This is assumed to be the adiabatic value. Such a procedure is only justified within a few hundred metres of cloud base. **This method produces a cloud base around 465 m for run 1B and 510-575 m for run 2A. The bases finally chosen are shown below. The higher bases assumed for runs 8A, 8B will be discussed briefly later.**

Run Number	1A	1B	2A	2B	3B	8A	8B
Base (m)	400	450	500	525	575	675	750

The cloud base temperature was in the range 8.5-10.5°C.

3.3 Specification of Cloud Entry and Exit

The J-W zero-level signal undergoes a low frequency drift with time and it also contains a high frequency noise component of variable peak amplitude. In order to overcome the former problem the J-W data is plotted out for each run and a mean zero estimated which is subtracted from each data point in that run during the subsequent analysis. The latter problem is illustrated in Figure 1 which shows baseline noise with a peak amplitude of 0.03 gm^{-3}. This is a severe case and later on the amplitude fell below 0.01 gm^{-3}. The reason for this variation is not known.

The baseline noise makes it difficult to define the cloud boundaries during computer analysis unless all liquid water contents less than about 0.025 gm^{-3} are discarded. To overcome this problem the cloud boundaries have been

determined from the ASSP liquid water contents, using a critical value of 10^{-3} gm^{-3}. Whilst this may seem rather low, inspection of the 1s data by eye shows that the cloud boundaries are extremely well defined. There are few ASSP liquid water contents in the range 3×10^{-4} gm^{-3} to 10^{-2} gm^{-3}, so that typically at the cloud boundary a liquid water content of 2×10^{-4} gm^{-3} is followed by a value of 0.01 gm^{-3} (within cloud). Although this procedure will produce some error in the statistics for the 0–0.05 gm^{-3} range, this appears inevitable and the generation of many spurious values within this range is avoided. The affect of varying the critical ASSP liquid water content is explored later.

3.4 Results

The statistical distribution of liquid water content is plotted in Figure 2 as a function of height above cloud base. The statistics shown are the maximum and mean values plus the values of liquid water content below which lie 90%, 75%, 50%, 25% of the observations. Figure 3 shows the same data converted to a percentage of the adiabatic value. The percentage of adiabatic liquid water content appears to decrease with height. The smoothness of the hand-drawn curves is rather deceptive because of the lack of data between 300 and 970 m. Also the highest run only contains 34 data points. Runs 8A and 8B (plotted at 270, 190 m on Figures 2 and 3) were originally processed using cloud bases of 550 m and 650 m respectively. However the maximum liquid water contents were then found to be around fifty per cent of the adiabatic value which seemed rather low for a level of a few hundred metres above cloud base in a non-precipitating, non-glaciated cloud. The values finally chosen assume that the maximum observed value is the adiabatic liquid water content. Whilst this argument is rather incestuous it reflects the uncertainty in cloud base height for the later runs, since profile 2 gave a cloud base of 500 m prior to run 8A and profile 3 gave 690 m at the end of run 8B.

The operation of the criterion for being in cloud is explored in Figures 4 and 5. Histograms of liquid water content for runs 1A and 8B are shown in Figure 4. The solid histogram results when J-W values are chosen for ASSP liquid water contents greater than 10^{-3} gm^{-3} whilst the dotted and dashed histograms used 5×10^{-2} and 10^{-2} gm^{-3} respectively. Run 1A appears more sensitive because it contains far fewer data points than run 8B. The operation of the rejection criterion is examined in detail in Figure 5, which is a high resolution plot of part of run 1A from 1004.40–1005.57 GMT. The liquid water content from the ASSP (dashed line) and J-W

are superimposed. The horizontal bars at the top delineate the accepted values for the three criteria. The extra values rejected going from 10^{-3} to 10^{-2} gm^{-3} are marked by arrows. By comparing Figures 1 and 5 it can be seen that the J-W baseline noise is small between 1004.40 and 1004.55. However the increase in J-W signal after 1005.50 appears to be due to noise because the ASSP liquid water content was 10^{-4} gm^{-3} and the dew point depression 3°C at this time. Figure 5 indicates that a limit of 0.01 gm^{-3} may be leading to the rejection of real cloud data eg at 1004.56 and 1005.58. Although the rejection value of 10^{-3} gm^{-3} used so far performs quite well it may be safer to use 5×10^{-3} gm^{-3} for subsequent work. However it should be born in mind that the J-W liquid water contents are about twice as large as the ASSP values on average, for reasons as yet unknown. If this ratio were to change significantly then a different value for the rejection criterion may be required.

Examples of the cloud drop-size distribution, normalised to a peak value of unity are shown in Figure 6a. The unbroken distribution (run 2B) was obtained 150 m above cloud base with liquid water content 0.06 gm^{-3} and concentration 30 cm^{-3} and the dotted distribution (run 3A) at 950 m with liquid water content 0.3 gm^{-3}, concentration 55 cm^{-3}. The latter is an interesting example of a bimodal distribution and also illustrates the broadening of the distribution with height. The dashed distribution (run 3B), also obtained 950 m above cloud base, seems to belong to a different population because the drop concentration was 250-300 cm^{-3}, hence the low mean radius despite the liquid water content of 0.15-0.3 gm^{-3}. It is possible the updraughts were much more vigorous in the latter case but it is beyond the scope of this study to investigate the cloud dynamics.

4. Isolated Cumulus Study H496 11 February 1982

4.1 Meteorological Conditions and Flight Plan

The flight was undertaken to study the influence of turbulent mixing on drop-size distributions in isolated medium sized cumulus. On this day the operating area was to the southwest of the Scilly Isles. Two cold fronts were moving eastwards over the United Kingdom with an unstable airstream behind and a trough orientated N-S over Ireland. To the south of Ireland convection was less rigorous and according to the flight log there were no showers in the operating area and little sign of glaciation. The 2-D probe data has not been processed to confirm this. The cloud bases were reported to be around 1000 m, temperature 0°C and tops 2200-2400 m, temperature -9°C. During the analysis few tops were found above 2000 m, -6.3°C.

Isolated moderate sized cumulus were selected and six penetrations of each cloud were attempted. These were near cloud base, mid level and near cloud top for the centre of the cloud and towards the edge of the cloud. 'Clear air' runs were also performed which sometimes encountered cloud and some of the clouds decayed before the runs were complete.

4.2 Determination of Cloud Base Height

Assuming that the maximum liquid water content value near cloud base represented the adiabatic value, the low level runs give a mean base height of 1030 m, range 1010-1075 m. The aircraft scientist reported the cloud bases to be at 1070 m which becomes 1040m after correction for the difference between altimeter and program pressure heights. The analysis program has been run for a base height of 1030 m. Because of the localised nature of the working area and the short runs there should be a negligible error due to variations in surface pressure.

4.3 Results

Initially the analysis was performed for runs located horizontally at the cloud centre. Later this was extended to include edge runs and 'clear air' runs which actually encountered cloud. Figure 7 shows the maximum and mean liquid water content plotted as a function of height above cloud base. Since several runs were performed at a given height the means in Figure 7b are for all data at a given height. In Figure 8 the liquid water contents have been converted to a percentage of the adiabatic value. The diagonal bars on the maximum values at 350, 940 m on Figure 8a delineate the error for a $\pm$ 50 m uncertainty in cloud base. Not surprisingly using all the data reduces the mean values but has little effect on the maximum values. On average 16 data points were obtained on each run so that statistics other than the mean and maximum have not been considered on a run basis. This is the main disadvantage of the individual cumulus flight plan.

Figure 6b shows the normalised drop size distribution as a function of height (the distribution near cloud top is from a different cloud to the other two). The mode radius increases with height and the distribution broadens. The drop concentration was about 50 cm^{-3}. Considering the reported absence of glaciation and precipitation this suggests a low CCN concentration which would be compatible with the synoptic situation. An individual LWC histogram has not been shown because of the limited data at each level.

5. KONTUR Flight H474 14 October 1981

5.1 Meteorological Conditions and Flight Plan

H474 was undertaken to study open cells over the German Bight. The operational area was to the rear of a nearly stationary low over Scandinavia. Cold air of polar origin (surface air temperature $\simeq 8^{\circ}C$) moved over the warm $\approx 14^{\circ}C$ North Sea resulting in the development of cumulus, cumulus congestus and an occasional cumulonimbus. An open cellular structure was apparent from the satellite photograph but during the flight such structure was only obvious over part of the operational area. Cloud base was reported around 1000 m but cloud top height was more variable. Generally tops were around 2400 m with a few Cu Cg tops to 3000 m. In some areas convection was suppressed with tops around 1800 m. Cloud base temperature was zero and the tops were around $-11^{\circ}C$. Significant glaciation was reported especially towards cloud top and moderate showers were encountered. This represents the most significant difference from the other two cases analysed.

The flight plan was identical to H463 except that all the profiles were performed at the southern end of the area. Cloud bases on profiles 1 and 2 were reported at 920 m, 1000-1070 m respectively and a correction of +70 m has been used for agreement with the MRF1 program pressure heights. During the analysis a cloud base of 1000 m has been used for the earlier runs and 1140 m for the rest. Finally note that according to the aircraft scientist's log the cloud base lowered to 600 m in showers, although this report was made en route to the operational area.

5.2 Results

The data has been analysed in a similar manner to H463 except that the ASSP was non-operational on runs 2.2 and 3.1. Cloud boundaries have been delineated by time for these cases. This is possible because of the limited number of cloud penetrations. Figure 9 shows the maximum and mean liquid water content as a function of height above cloud base, both in absolute terms and as a fraction of the adiabatic value. Although it is difficult to draw conclusions from the limited number of data points, the liquid water contents in Figure 9 seem similar to the other days despite the partial glaciation of the clouds. Low values of mean and maximum liquid water content can be seen at 1500 m above cloud base (runs 4.1, 4.2). As shown later the highest ice content was measured here by the 2-D probes.

On runs 2.1, 6.1, 6.2 taken to be 170 m above cloud base the maximum liquid water contents were $2\frac{1}{2}$ to $3\frac{1}{2}$ times the adiabatic value. They would represent the adiabatic value if the cloud base were 200 to 400 m lower.

This is compatible with the reported variation in showers.

The histograms of liquid water content are either similar to Figure 4 or exhibit a 'tail' of large values. In the latter case there are too few points to accurately define the shape of the tail and they are not reproduced here. The drop size distributions are also not shown because the intermittent ASSP fault and the presence of ice casts some doubt on their accuracy. Within 200 to 600 m of cloud base the mode radius was 7-12 μm with concentrations of 100-200 cm^{-3} (ASSP value x 2 for agreement with J-W). Little data was obtained at mid-levels whilst at 1500 m above cloud base the spectra were either narrow with a mode radius of 5 μm or very broad with multiple peaks between 5 and 18 μm.

The possibility exists that the J-W or ASSP do not define the cloud boundaries because of extensive totally glaciated regions. In order to examine this, 10s mean values of ice content from the 2-D probes have been compared with 10s mean J-W liquid water contents for all runs. It is clear that all significant ice contents ($> 0.01\ gm^{-3}$) occur within the cloud as defined by the J-W. Examples are shown in Figure 10 for run 3.2 (cloud base + 1 Km) and run 4.1, 4.2 (cloud base + 1.5 Km). Runs 3.2, 4.2 and most runs not illustrated show a clear anticorrelation between liquid water and ice contents. The main exception to this is run 4.1 which also illustrates the open cell structure. A brief examination of the vertical velocity data has shown that the largest peaks in liquid water content are in regions with the strongest updraught, up to 6 ms^{-1}. Such a vertical velocity is associated with the right hand peak in liquid water content on run 3.2. In contrast the more glaciated region illustrated for run 4.1 is associated with updraughts of less than 2 ms^{-1}. These observations are consistent with previous work which indicates that only the strong cooling within an updraught can generate sufficient condensation in the liquid phase to maintain the cloud liquid water against depletion by glaciation. Also where the updraught is strongest the cloud is likely to be in its formation stage and glaciation will not have had time to become established eg Matejka et al (1980).

6. Synthesis of Results

Although each cumulus flight has been analysed separately, as were the Sc flights, it is clear that insufficient data was gathered on each occasion to produce separate statistics for each day. Therefore the data has been combined in two ways. Firstly the maximum and mean liquid water contents, expressed as a fraction of the adiabatic value, have been plotted as a function of height above cloud base in

Figure 11. Also included on this diagram are a few values from flight H473 (13 October 1981) during which the meteorological and cloud conditions were extremely similar to H474. Despite the scatter there is a clear trend discernible in Figure 11 for the fraction of adiabatic liquid water content to decrease with height above cloud base. Warner (1970) has summarized several published studies of the variation of liquid water content with height in cumulus clouds and his own results are reproduced as the curve on Figure 11. Since this falls in the middle of the range of data which he has summarized, it appears that our values are slightly on the low side of previous work.

Because of the number of previous study it is not clear how much new information is contained in Figure 11 apart from the fact that it relates to the area of interest to us personally. In an attempt to extract more information our observations have been combined to produce histograms of the fraction of adiabatic liquid water content for 200 m layers above cloud base and these are shown in Figure 12. In order to produce this diagram and Figures 13, 15 the three runs from H474 which produced maximum liquid water contents which were significantly superadiabatic have been reprocessed with the cloud base lowered by 250 m–400 m. Even so a small fraction of superadiabatic liquid water content is still present in the statistics for the lowest two layers and this represents the uncertainty in cloud base. Figure 12 shows that the fraction of adiabatic decreases slowly with height. This is most noticeable above 1200 m where all the data originates from the most glaciated region of H474. Care must be taken in interpreting trends in the histograms because of the small number of observations at some levels eg 200–400 m, 1200–1400 m. No data was obtained between 400 and 600 m. Figure 12 also shows all the data combined into one histogram. The histograms have been converted to cumulative distributions which are shown in Figure 13a. Figure 13b merely shows the overall range of the distributions up to 1 Km above cloud base and thus provides a crude summary of the data.

7. Classification of the Liquid Water Content Distribution by Temperature

Khrgian (1963) has summarised extensive measurements of layer cloud liquid water content made in the USSR. He presents these as the percentage of liquid water content in 0.05 gm^{-3} classes from 0 to 1.6 gm^{-3}, for 5°C temperature intervals from +20 to -20°C. Roach has shown that these distributions can be approximated by:-

$$\log_{10} P(q) = -kq$$

where q is the liquid water content in gm^{-3} and $P(q)$ is the fraction of liquid water contents observed to be larger than q. Over the temperature range 0 to $-15^{\circ}C$ k increases with temperature and this variation has been fitted by Roach using the expression $k = 5 - T/3\ (^{\circ}C)$. Presumably $P(q)$ decreases at lower temperatures because of the decreasing adiabatic value and because of glaciation.

The cumulus data (excluding flight H473) has been reanalysed in terms of temperature alone, to look for a similar relationship. Figure 14 shows a log-linear plot of $P(q)$ against q. The number of 1s data points is also shown and it can be seen that there will be a large statistical uncertainty for $P(q)$ values less than 0.01. The data spans the temperature range +10 to $-15^{\circ}C$ but most was obtained at temperatures above $-5^{\circ}C$. It can be seen from Figure 14 that the relationship is reasonably linear for the temperature ranges 5 to $10^{\circ}C$ and -5 to $-10^{\circ}C$ but not for the other two ranges. Furthermore the probability of obtaining higher liquid water contents increases with decreasing temperature down to $-10^{\circ}C$. Bearing in mind that the cloud base temperature was $0^{\circ}C$ for H474, H496 and $10^{\circ}C$ for H463, it is clear that this represents the influence of height above cloud base. All the data in the 5 to $10^{\circ}C$ range comes from H463 and Figure 2 shows that this was mainly obtained within 300 m of cloud base. The probability decreases again below $-10^{\circ}C$. This data comes from H474 above 1200 m and genuinely reflects the influence of glaciation.

It is clear that this type of analysis needs a large number of clouds with different base temperatures to be sampled, so that data from many levels above cloud base are included in each temperature category. This conclusion has been confirmed by reanalysis of our Sc observations in terms of temperature alone.

Finally the cumulative distributions in Figure 13 have been plotted in log-linear form in Figure 15. The relationship is not particularly linear in this form but there is a considerable reduction in scatter compared to Figure 14.

8. Conclusions

The multiplicity of forms of analysis described here are part of a learning process and they would not all be repeated in future work. The best form of presentation appears to be that in Figure 12 or 13, although 200 m may not be the optimum depth for averaging. Such a presentation allows data from many flights to be combined for statistical analysis. It naturally takes account of the increase in liquid water content with height implicit in the adiabatic concept. Depletion of cloud liquid water content by mixing and glaciation can also be taken into account when the data is stratified by height above cloud base. Allowance for glaciation could be refined further by stratifying the data by cloud base temperature. However this would probably require the accumulation of an

unrealistically large number of case studies.

Classification of the liquid water content by temperature alone produces more scatter than using the adiabatic concept. It seems likely that to smooth out the influence of height above cloud base even more observations would be required than would be necessary to produce sufficient data at each level in Figure 12.

Finally two problems not raised in this report may require some thought if further work is contemplated. One of these is the response of the J-W to precipitation sized drops and to ice crystals. For example in mixed conditions as shown in Figure 10, does the J-W signal contain a contribution from wet ice. Secondly are the 1s mean data used here statistically independent and if not does this matter when producing histograms as in Figure 12?

References

A Kh Khrgian (Ed) 1963 Cloud Physics
Isreal Programme for Scientific Translations.

T J Matejka, R A Houze Jr and P V Hobbs 1980 Microphysics and dynamics of clouds associated with mesoscale rainbands in extratropical cyclones.
Quart. J. R. Met. Soc., 106, 29-56.

P Personne, J L Brenguier, J P Pinty and Y Pointin 1982 Comparitive study and calibration of sensors for the measurement of the liquid water content of clouds with small droplets.
J. Appl. Met., 21, 189-196.

J W Strapp and R S Schemenauer 1982 Calibrations of Johnson-Williams liquid water content meters in a high speed wind tunnel.
J. Appl. Met., 21, 98-108.

J Warner 1970 On steady state one-dimensional models of cumulus convection.
J. Atmos. Sci., 27, 1035-1040.

Figure Legend

Figure 1 J-W (upper) and ASSP liquid water contents vs time for H463, run 1B, a period with a large J-W baseline noise signal.

Figure 2 Liquid water content distribution vs height above cloud base for H463, 23 September 1981. The liquid water content statistics plotted are the maximum (•) and mean (▪) values plus 90% (*), 75% (⊙), 50% (×) and 25% (•) of the observations less than the given liquid water content.

Figure 3 As Figure 2 except that the liquid water contents are expressed as fractions of the adiabatic value. Error bars for a ± 50 m variation in cloud base are shown on selected 90% data points.

Figure 4 Histograms of the percentage of liquid water content in 0.05 gm^{-3} width classes for H463. The histograms for three ASSP rejection criteria are shown ——— 10^{-3} gm^{-3}, ••••••• 5 x 10^{-2} gm^{-3}, – – – 10^{-2} gm^{-3}.

Figure 5 Plot of J-W •———• and ASSP ×– – –× liquid water content against time for H463, run 1A. The horizontal lines at the top delineate the J-W data points accepted using an ASSP LWC criterion of 10^{-3} gm^{-3}, 5 x 10^{-2} gm^{-3}, 10^{-2} gm^{-3}. The arrows indicate the data points rejected when the critical LWC is increased from 10^{-3} gm^{-3} to 10^{-2} gm^{-3}.

Figure 6 (a) Examples of normalised drop-size distribution from H463

•——— cloud base + 150 m, conc. 30 cm^{-3}, LWC 0.06 gm^{-3}, 14 sec mean.

×– – –× cloud base + 975 m, conc. 25-300 cm^{-3}, LWC 0.15-0.3 gm^{-3}, 11 sec mean.

o••••••••o cloud base + 950 m, conc. 55 cm^{-3}, LWC 0.3 gm^{-3}, 1 sec mean.

(b) Examples of normalised drop-size distribution from H496

×– – –× Cloud base + 50 m, LWC 0.05 gm^{-3}, 14 sec mean } conc.

o••••••••o Cloud base + 350 m, LWC 0.2 gm^{-3}, 6 sec mean } 50 cm^{-3}

•——— Cloud base + 950 m, LWC 0.2-0.4 gm^{-3}, 4 sec mean }

Figure 7 Maximum (×) and mean (•) liquid water content vs height for H496, 11 February 1982. (a) Cloud centre data (b) All data.

Figure 8 As Figure 7 except that the liquid water contents have been converted to percentages of the adiabatic value. Error bars for a ± 50 m variation in cloud base are shown in Figure 8a.

Figure 9 (a) Maximum (×) and mean (•) liquid water contents vs height for H474, 14 October 1981.

(b) As Figure 9a except that the liquid water contents have been converted to a percentage of the adiabatic value.

Figure 10 Ten second mean values of J-W LWC ——— and ice content from the 2-D Probes — — — — — plotted against time for several runs from H474.

Figure 11 Maximum (11b) and mean (11a) liquid water content as a function of height above cloud base combining all cases plus H473. The trend in mean LWC from Warner (1970) is reproduced as the dashed curve.

Figure 12 Histograms of the percentage of time vs percentage of adiabatic liquid water content for 200 m layers above cloud base, combining all cases plus H473. The number of 1s data points is shown for each histogram. The bottom right hand histogram results from combining the data at all levels.

Figure 13 (a) The histograms in Figure 12 are replotted as cumulative distributions i.e. the percentage of time for which a given percentage of adiabatic is exceeded.

(b) Summary of the range of values in (a) excluding the 1200-1400 m data.

Figure 14 Data from H463, H496 and H474 reanalysed in terms of 5°C temperature classes and plotted as the fraction of time $P(q)$ with liquid water content greater than q gm^{-3} for each class. The number of 1s data points in each class is also shown.

Figure 15 Cumulative distributions from Figure 13a replotted on a log-linear scale for comparison with Figure 14.

FIGURE 1 H463 RUN 1B 101800-104549

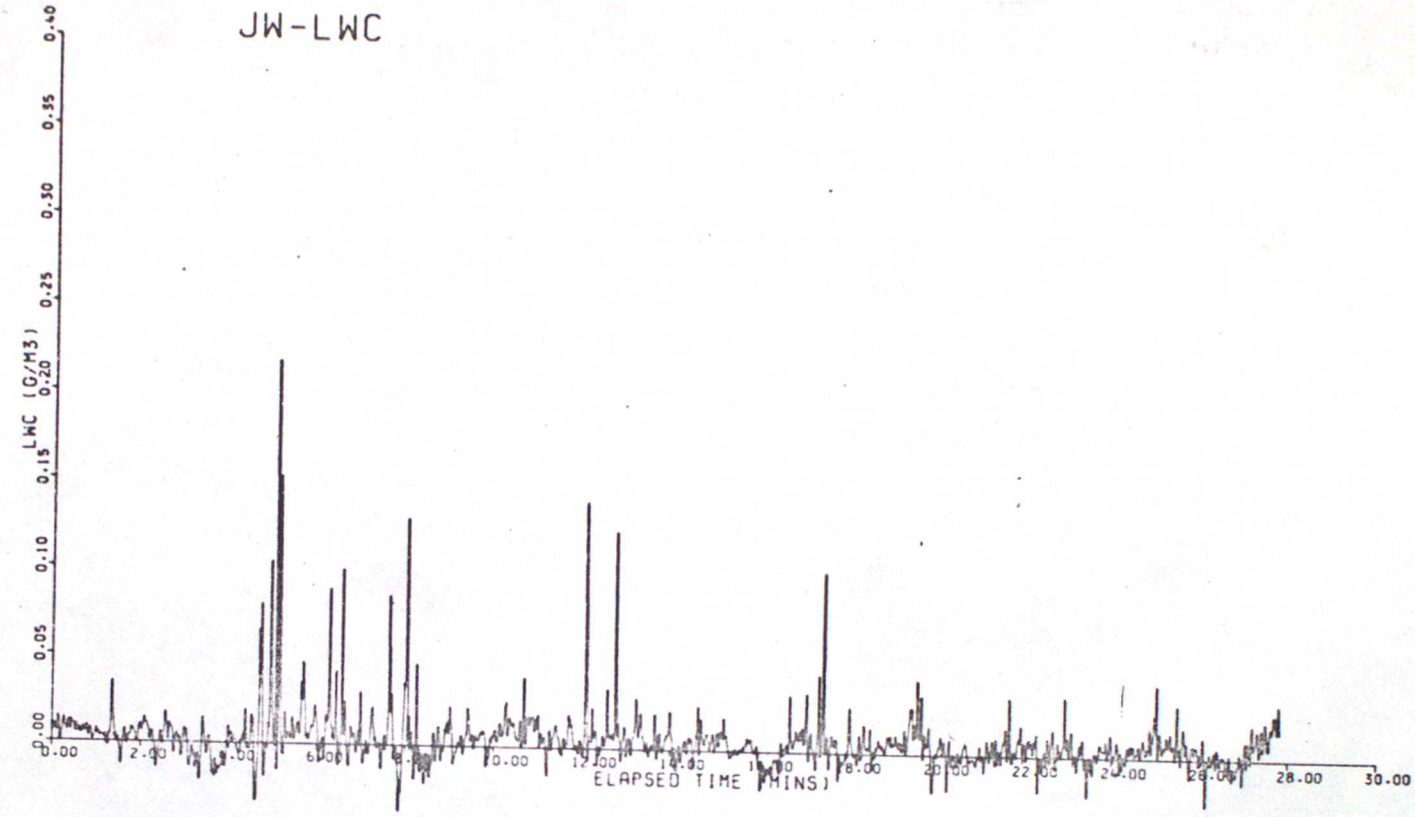

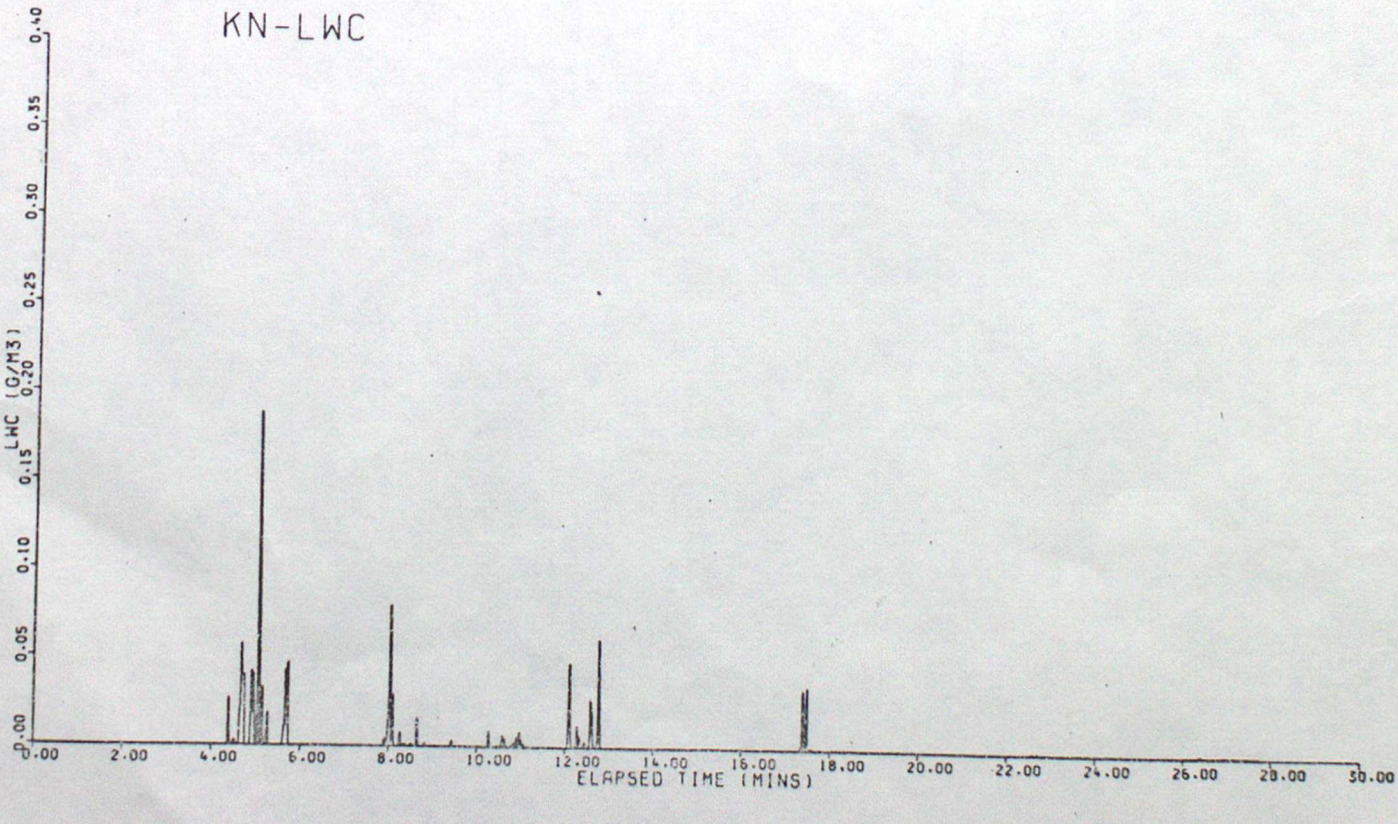

FIGURE 2

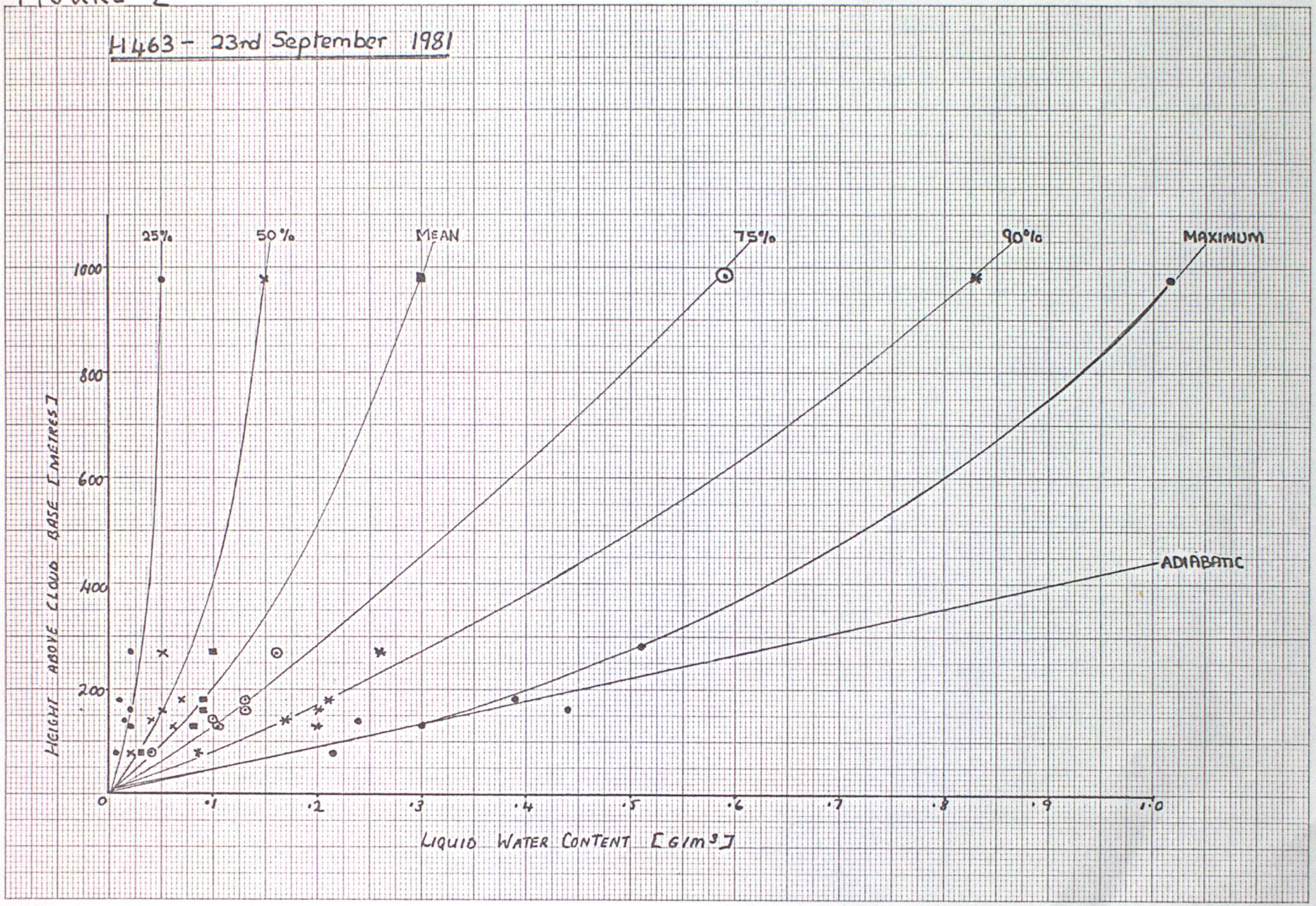
H463 - 23rd September 1981
25%
50%
MEAN
75%
90%
MAXIMUM
ADIABATIC
1000
800
600
400
200
0
·1
·2
·3
·4
·5
·6
·7
·8
·9
1·0
HEIGHT ABOVE CLOUD BASE [METRES]
LIQUID WATER CONTENT [GM M⁻³]

FIGURE 3

H463 - 23rd September 1981

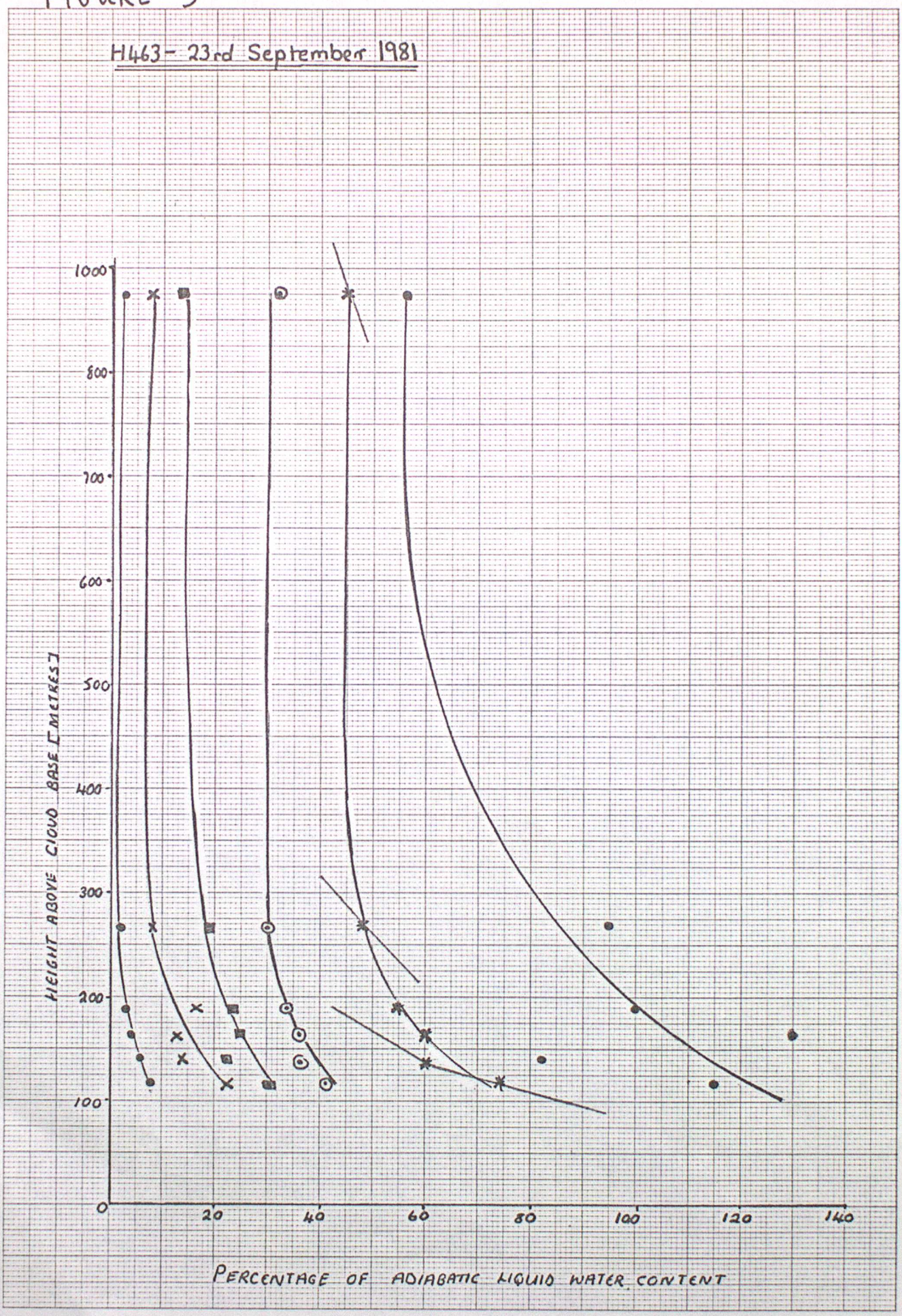

FIGURE 4 LWC DISTRIBUTIONS FOR H463

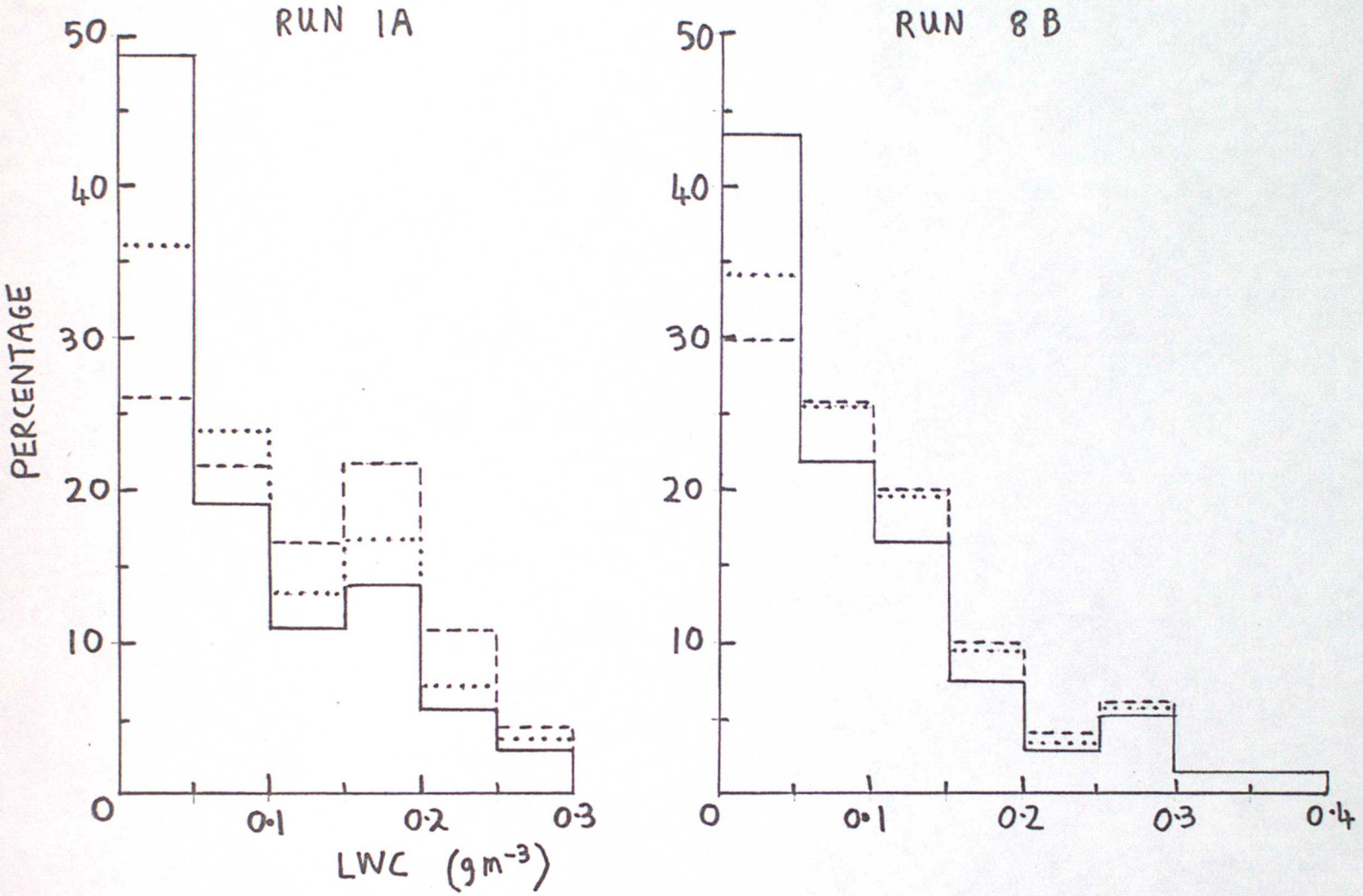

FIGURE 5 HIGH RESOLUTION PLOT TO ILLUSTRATE THE OPERATION OF THE REJECTION CRITERION

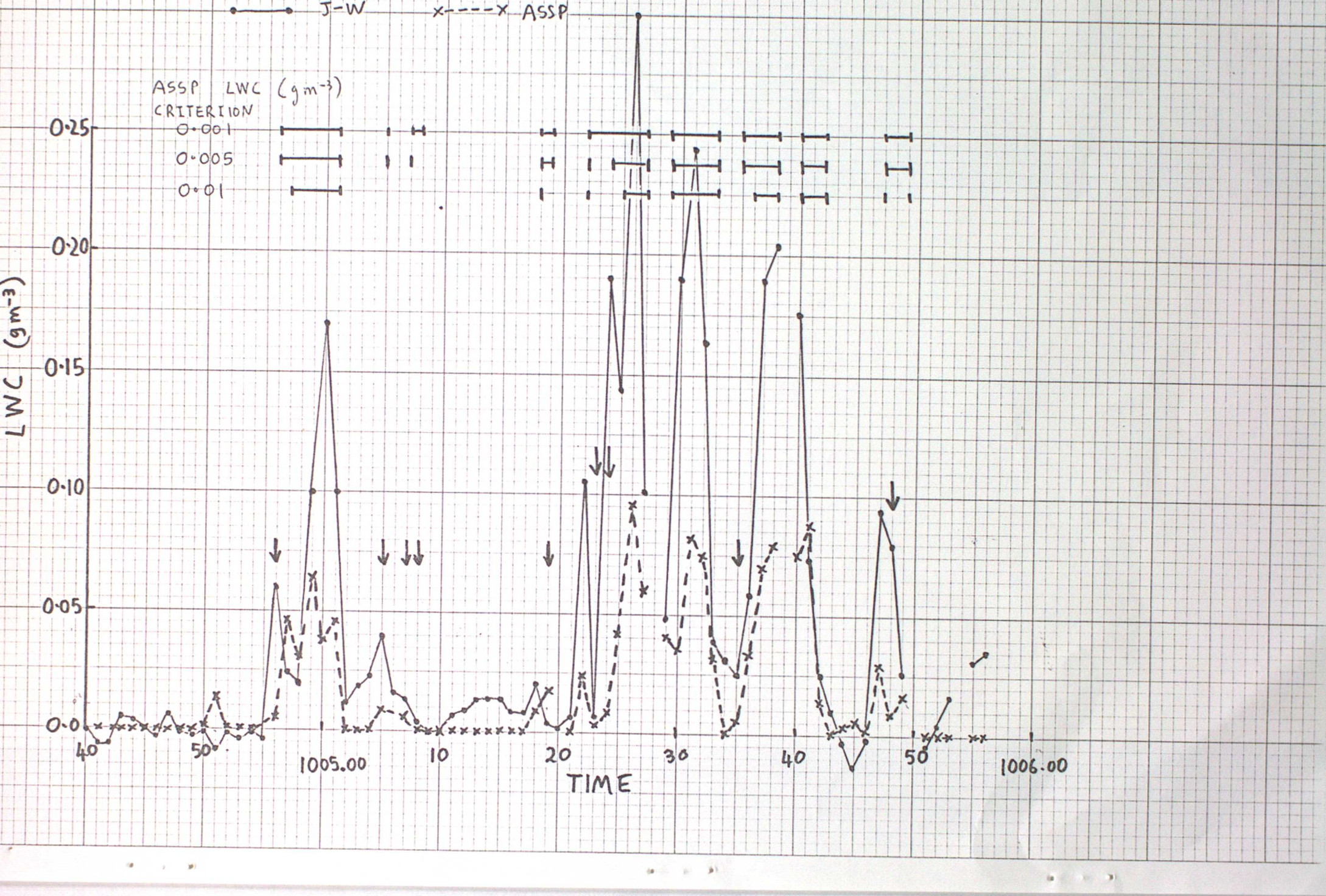

FIGURE 6 NORMALISED DROP-SIZE DISTRIBUTIONS

(a) H463

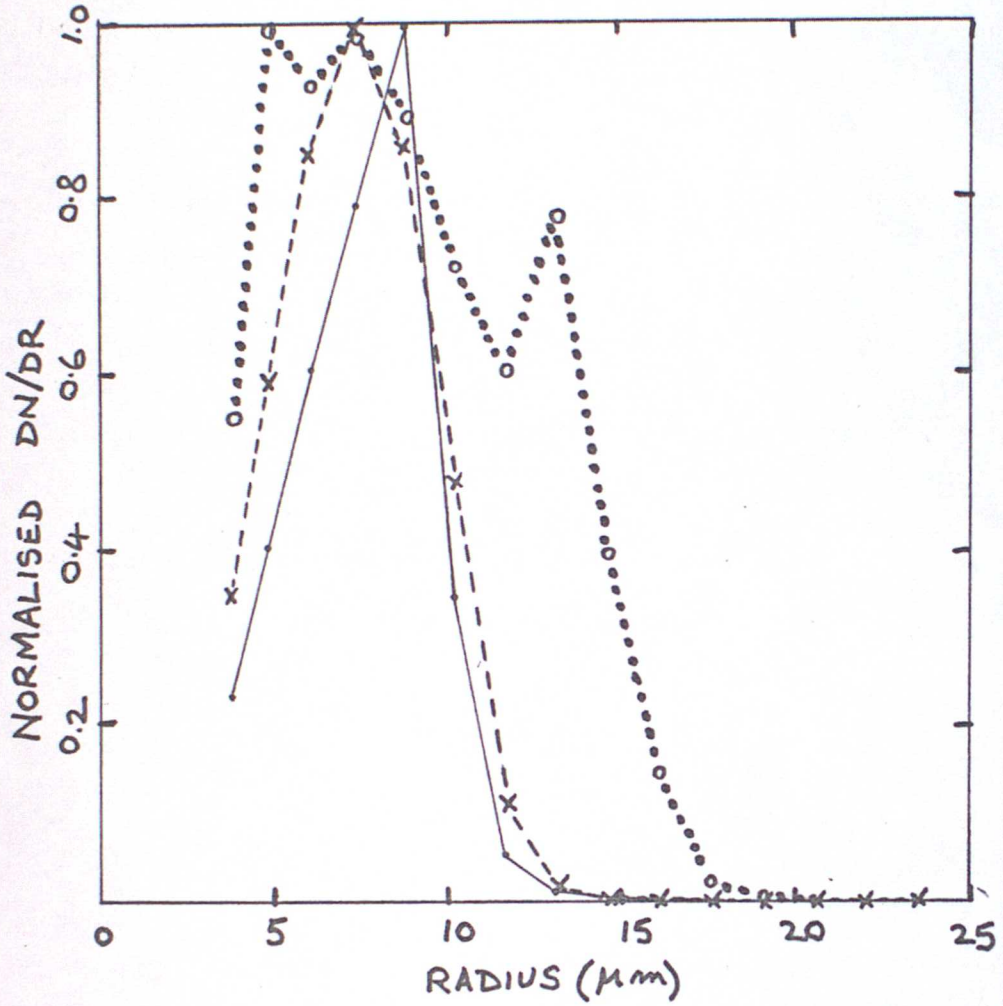

(b) H496

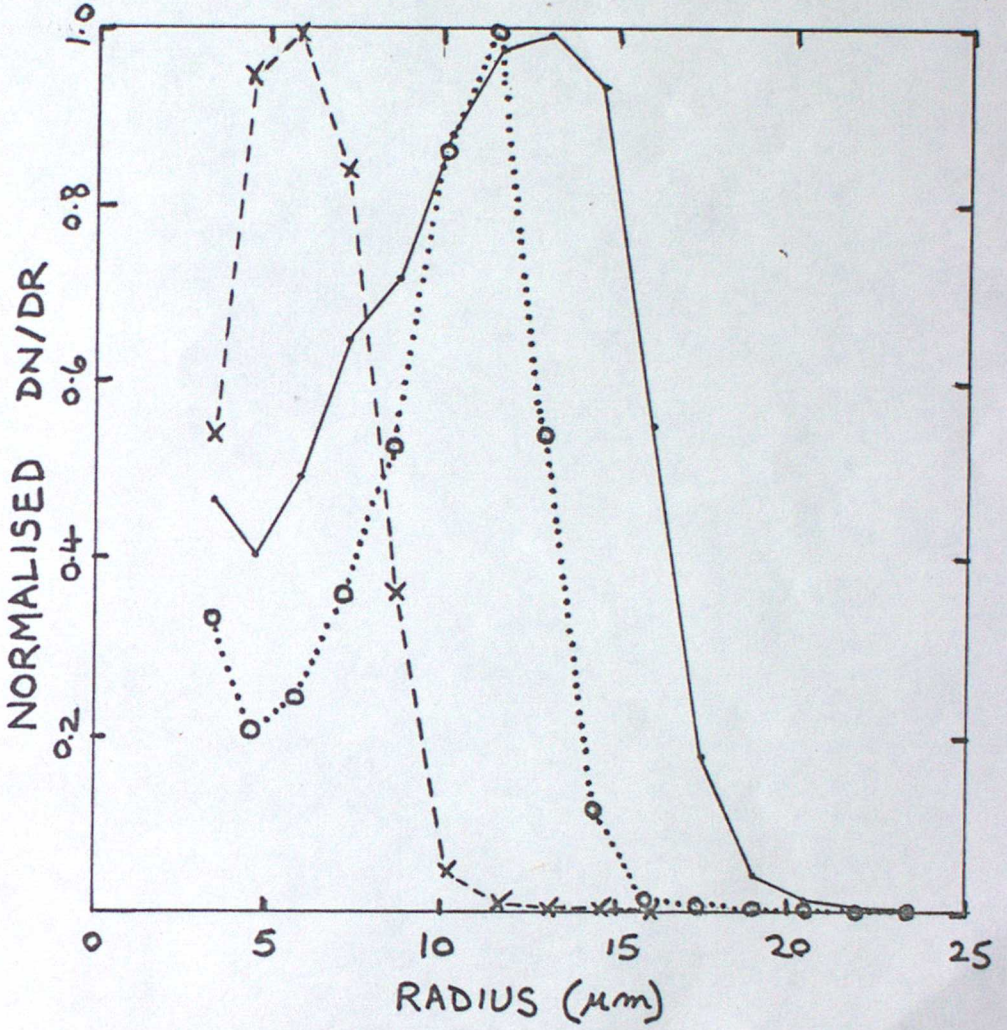

FIGURE 7 H 496

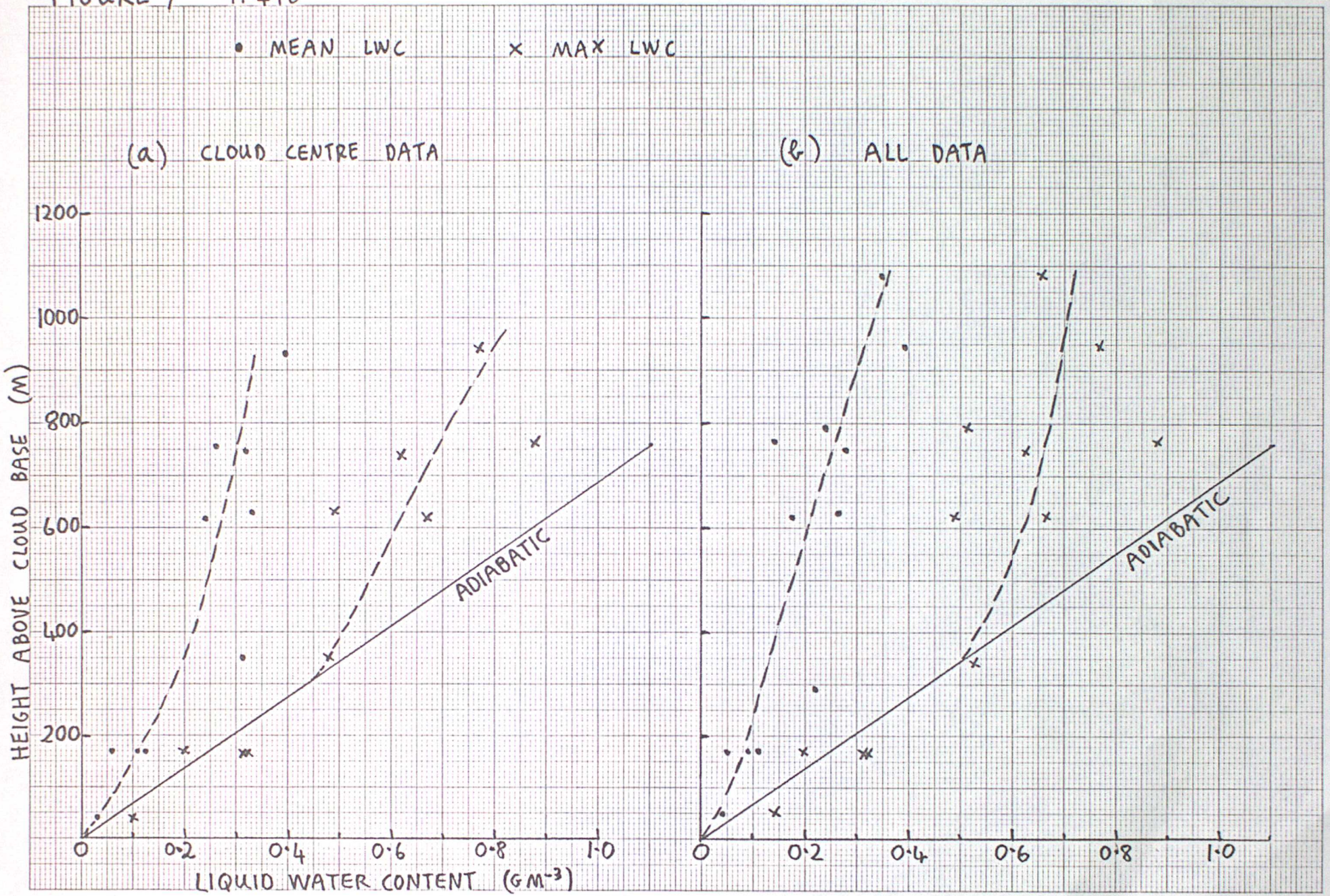

FIGURE 8 H496

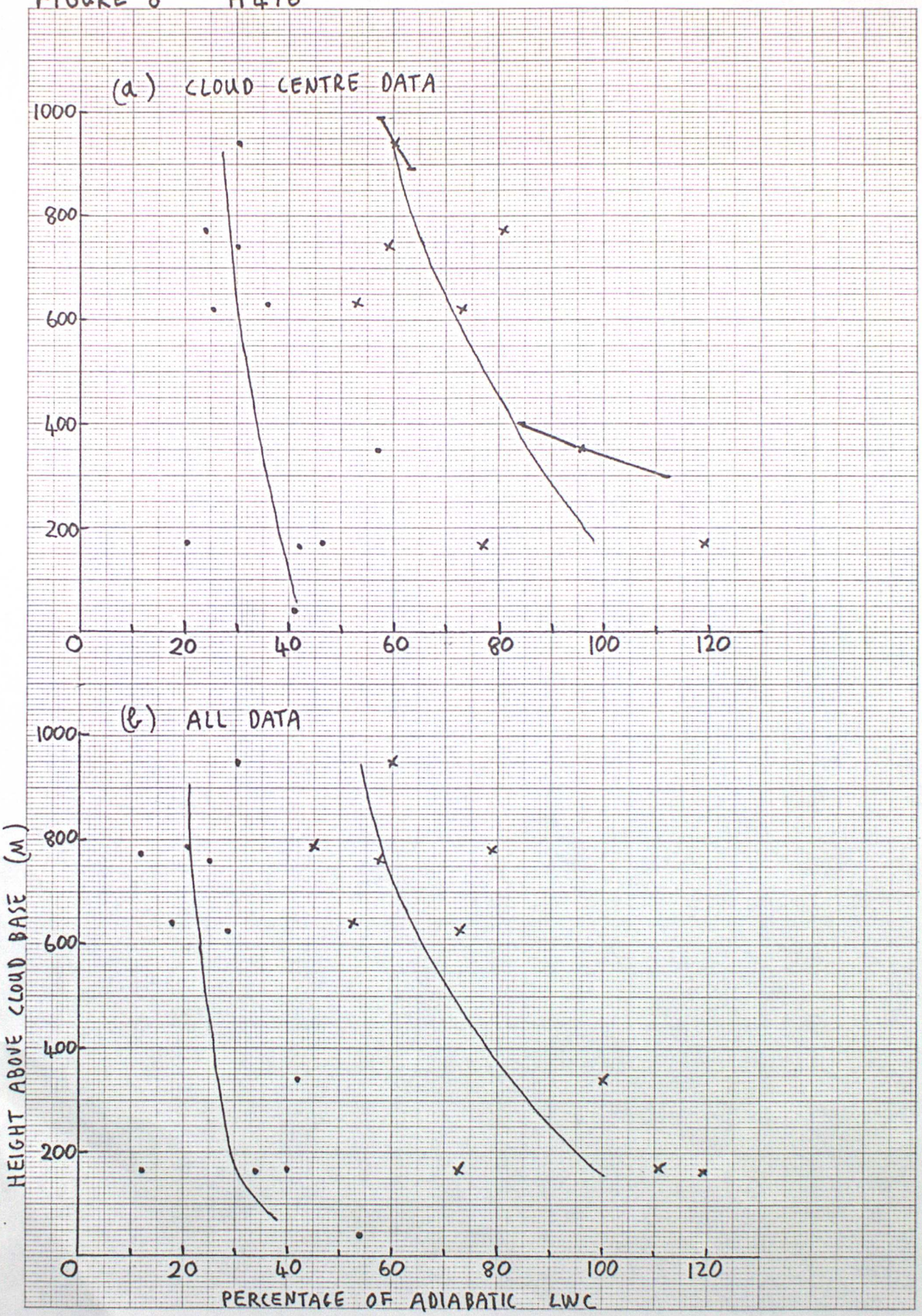

FIGURE 9 H474

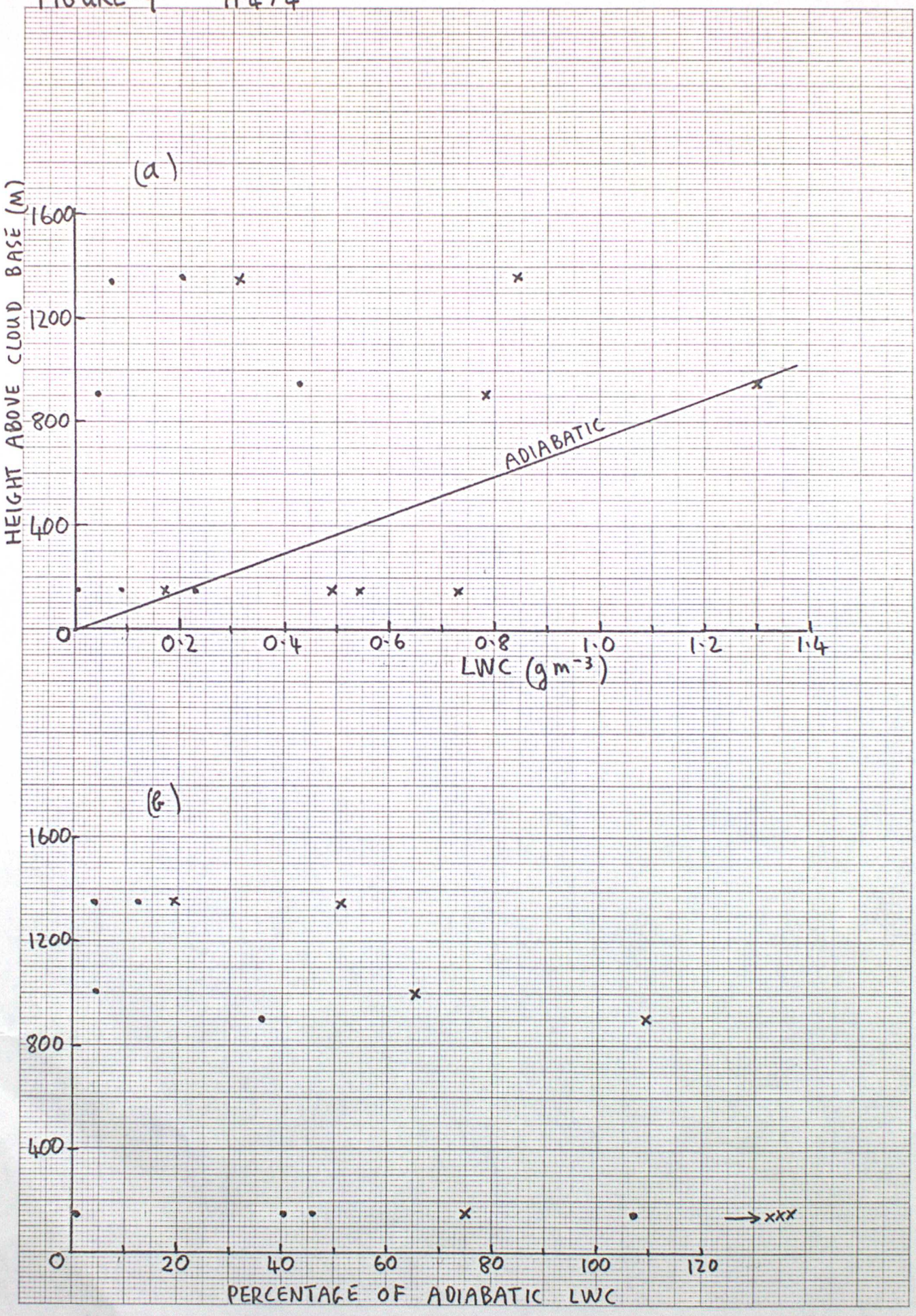

FIGURE 10 H474 —— J-W LWC --- 2-D PROBE ICE CONTENT

RUN 3.2 1207.50 – 1232.14

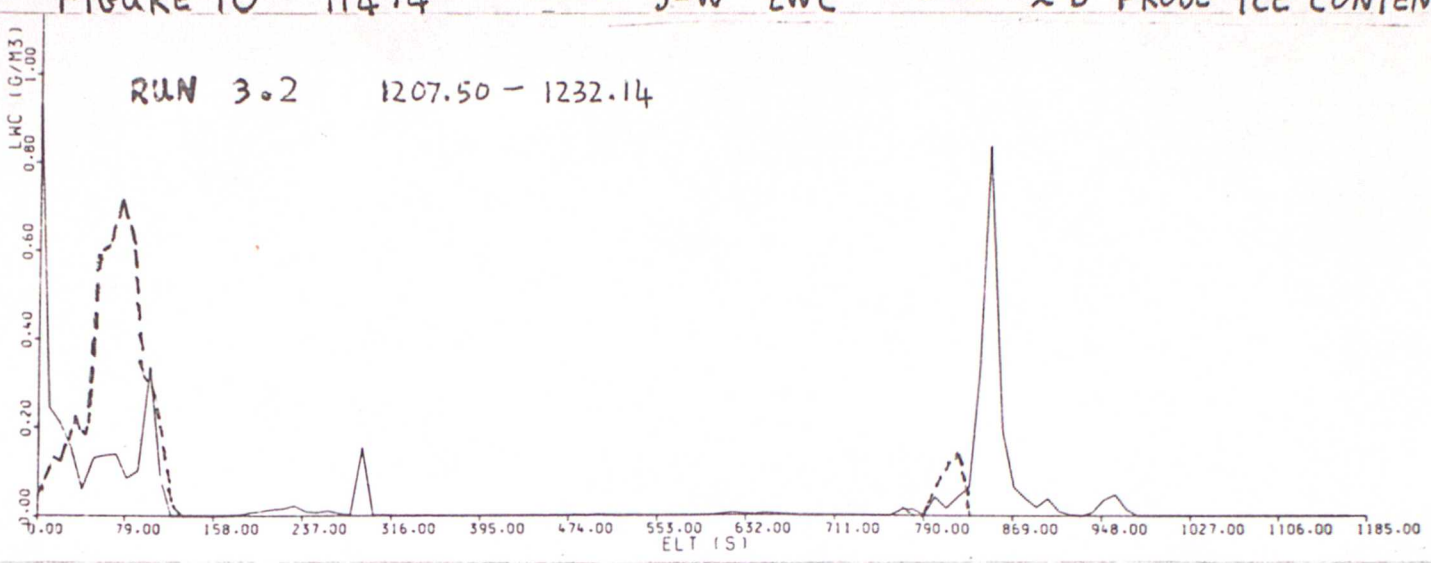

RUN 4.1 1236.01 – 1254.52

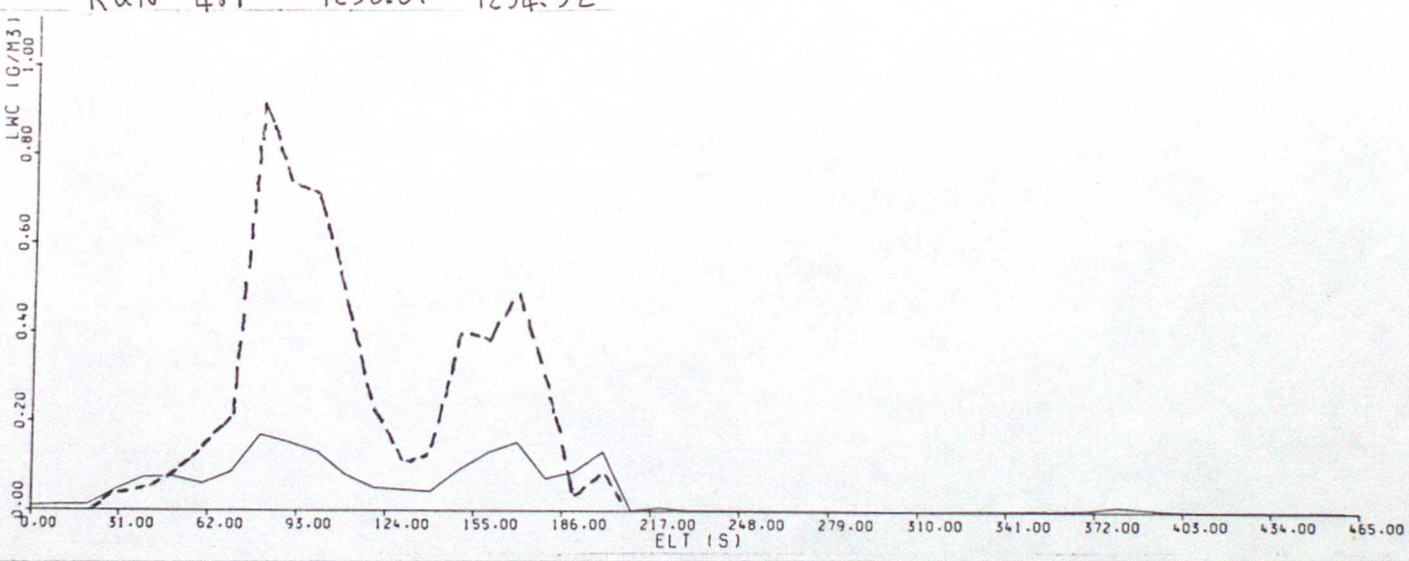

RUN 4.2 1256.19 – 1316.18

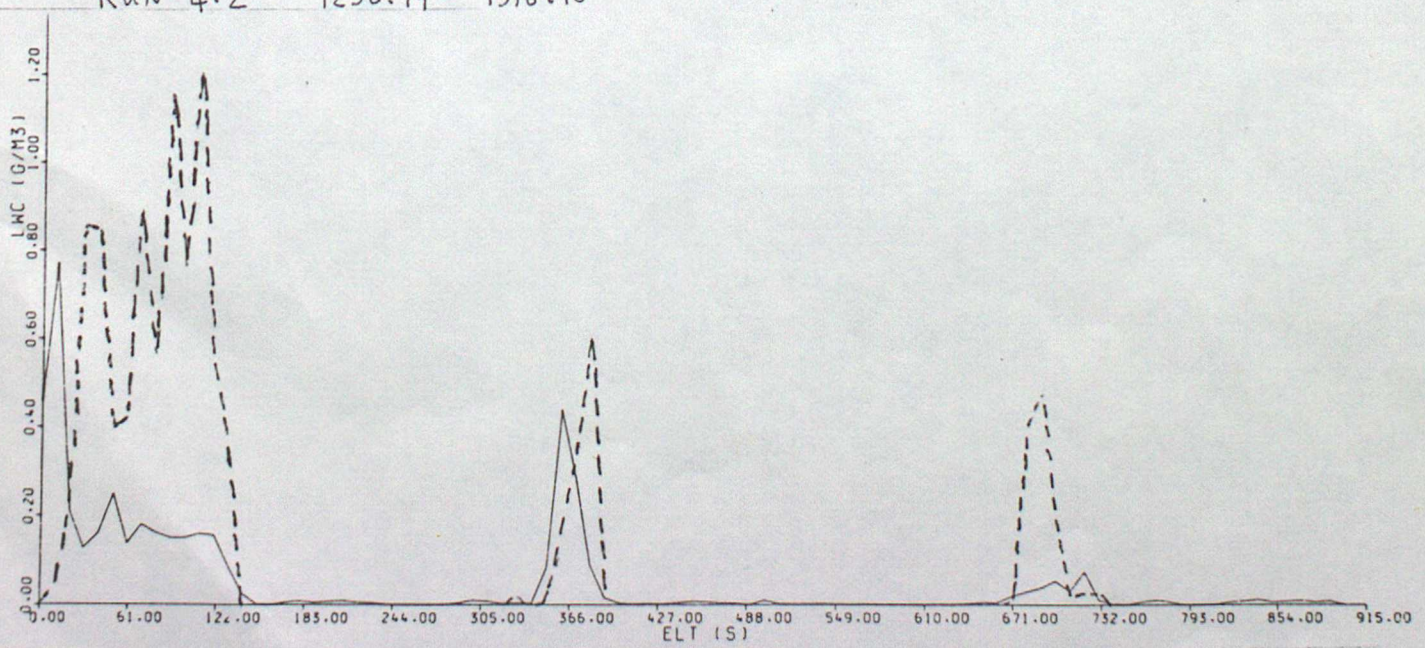

FIGURE 11 ALL DATA COMBINED ■ H473 ⊙ H474 + H463 ▲ H496

---- WARNER (1970)

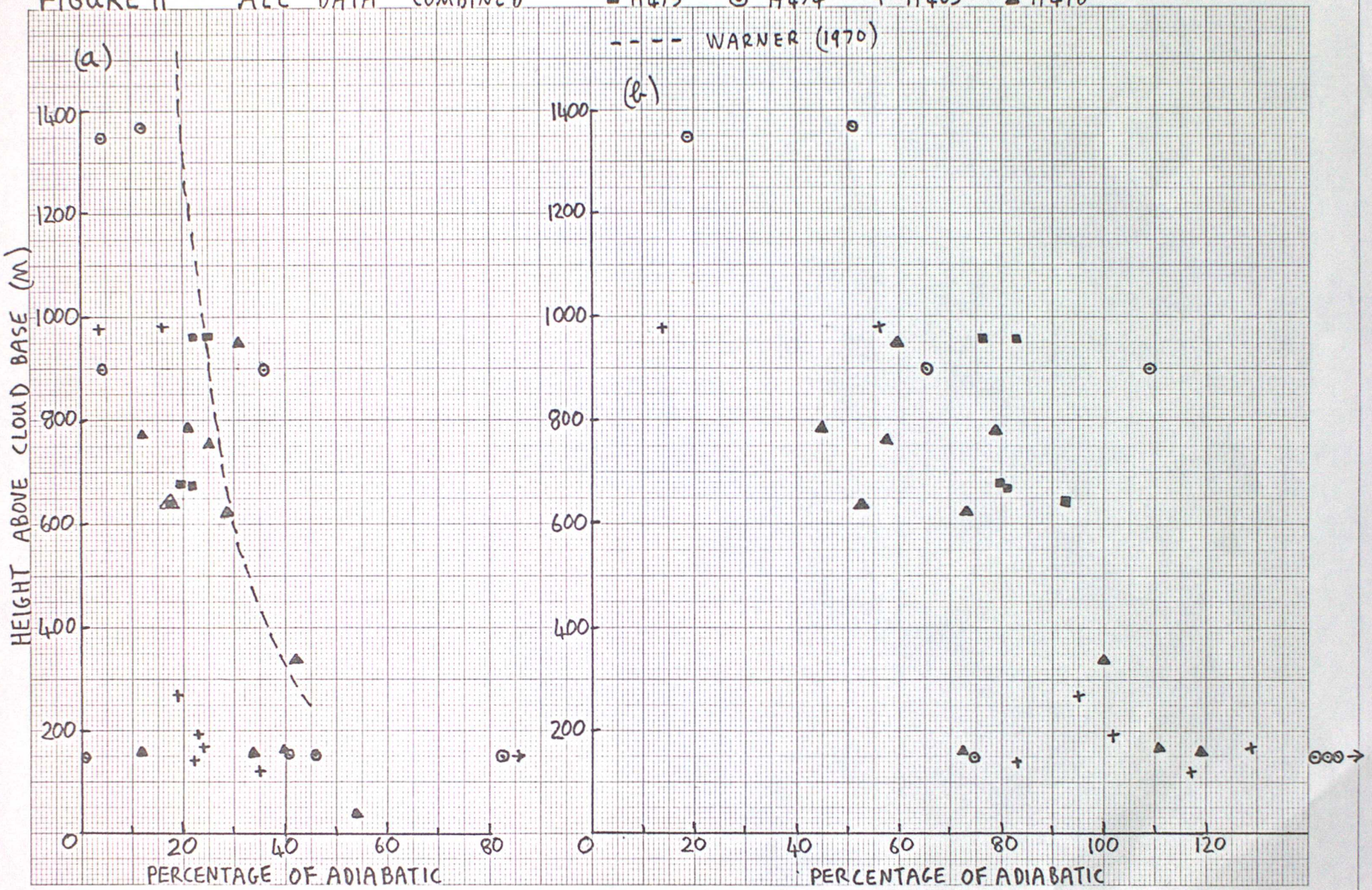

FIGURE 12 DISTRIBUTIONS OF FRACTION OF ADIABATIC LWC

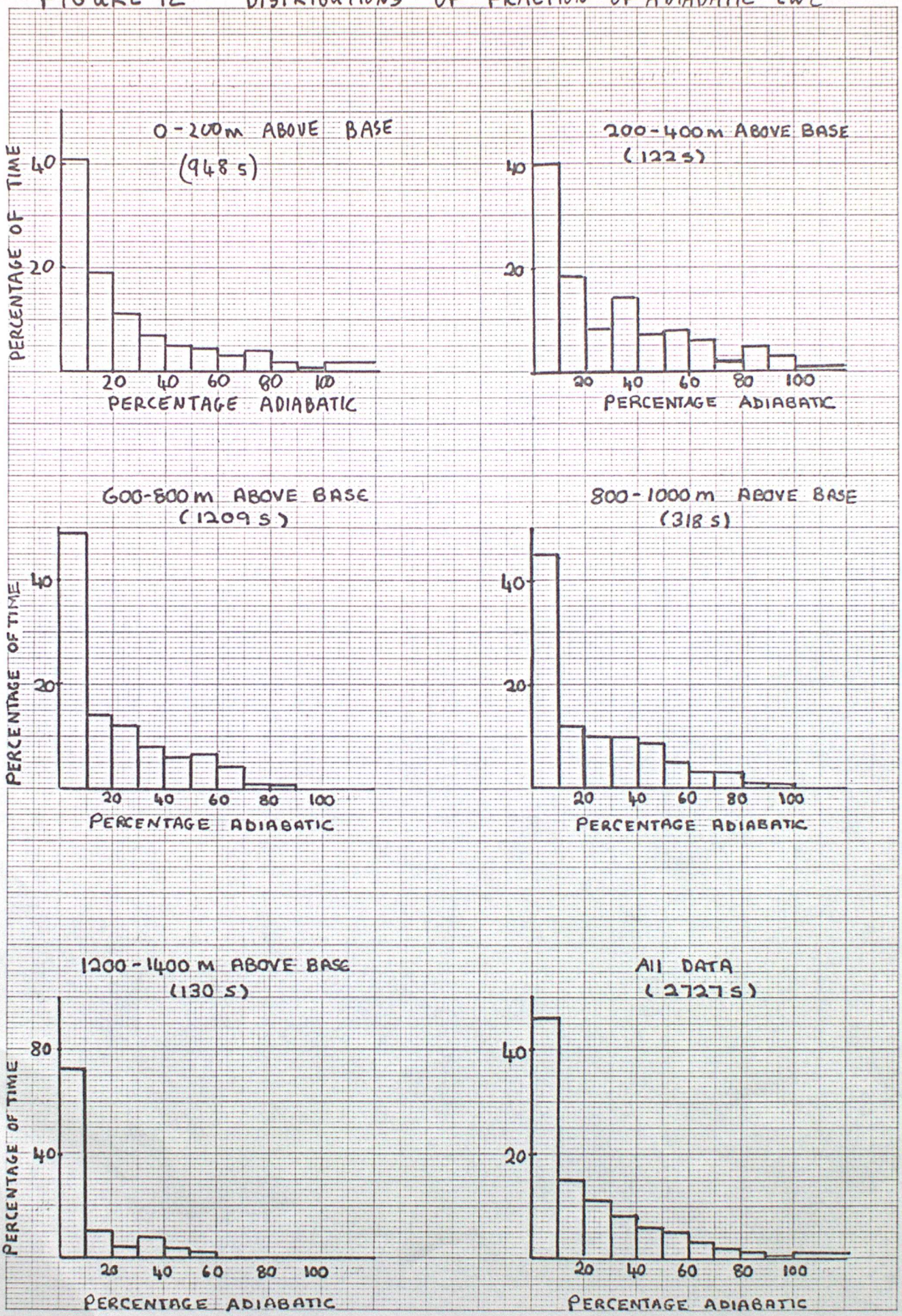

FIGURE 13

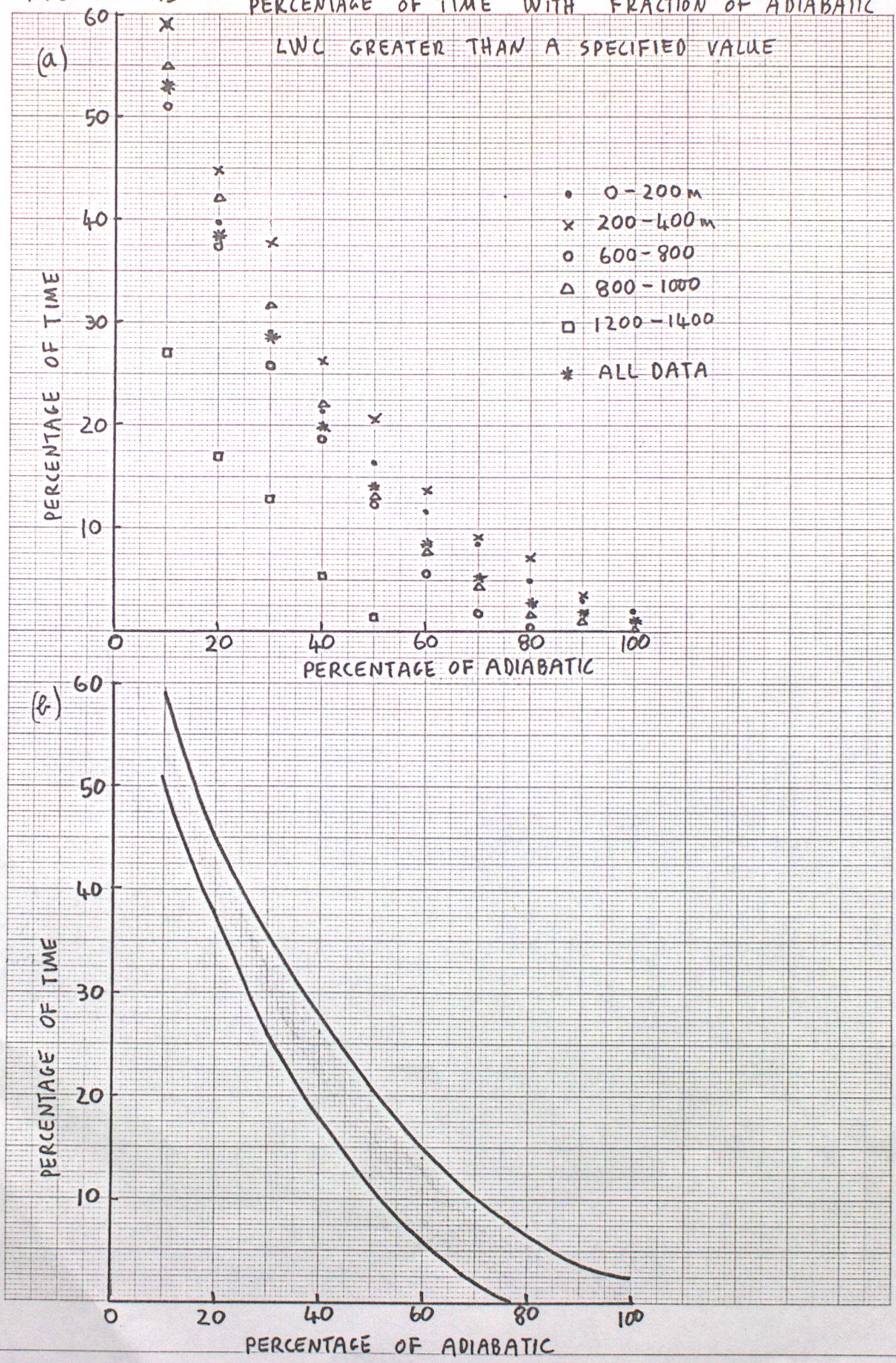
(a)
PERCENTAGE OF TIME WITH FRACTION OF ADIABATIC LWC GREATER THAN A SPECIFIED VALUE
PERCENTAGE OF TIME
60
50
40
30
20
10
0
20
40
60
80
100
PERCENTAGE OF ADIABATIC
0 - 200 m
200 - 400 m
600 - 800
800 - 1000
1200 - 1400
ALL DATA
(b)
PERCENTAGE OF TIME
60
50
40
30
20
10
0
20
40
60
80
100
PERCENTAGE OF ADIABATIC

FIGURE 14 FRACTION OF TIME WITH LWC GREATER THAN A SPECIFIED VALUE

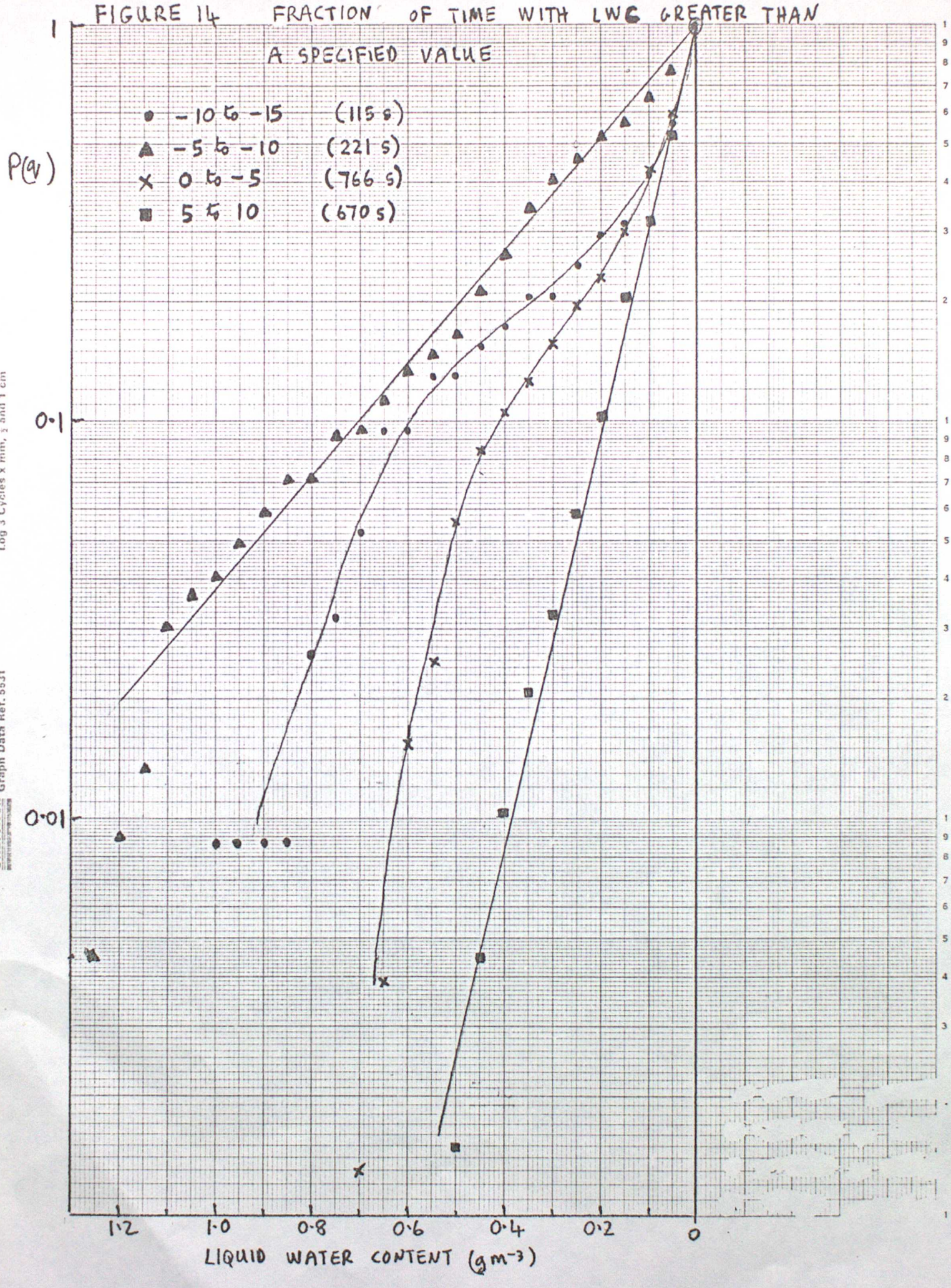

FIGURE 15 PERCENTAGE OF TIME WITH FRACTION OF ADIABATIC LWC GREATER THAN A SPECIFIED VALUE